

Quantum Pattern Recognition With Liquid State NMR

Rodion Neigovzen,^{1,2} Jorge Neves,³ Rudolf Sollacher,¹ and Steffen J. Glaser³

¹Siemens AG, Corporate Technology, Otto-Hahn-Ring 6, D-80200 Munich, Germany

²Physics Department, Technische Universität München,
James Franck Str., D-85748 Garching, Germany

³Department of Chemistry, Technische Universität München,
Lichtenbergstrasse 4, D-85747 Garching, Germany

(Dated: November 7, 2018)

A novel quantum pattern recognition scheme is presented, which combines the idea of a classic Hopfield neural network with quantum adiabatic computation. Both the input and the memorized patterns are represented by means of the problem Hamiltonian. In contrast to classic neural networks, the algorithm can simultaneously return multiple recognized patterns. The approach also promises extension of classic memory capacity. A proof of principle for the algorithm for two qubits is provided using a liquid state NMR quantum computer.

PACS numbers: 03.67.Lx, 03.67.Ac, 07.05.Mh, 82.56.-b

The framework of Natural Computing tries to model architectures found in Nature and to apply them to a diversity of computational tasks. Its biological domain is represented amongst others by neural networks and evolutionary computation. In physics, novel algorithmic schemes have been investigated in the context of quantum computation. Based on these ideas, we investigate how bioanalogue information processing like pattern recognition can be implemented on the nano scale.

Neural networks involve interacting units called neurons designed according to neural structures of a brain which cooperate in order to process information [1]. Similar to the brain, neural networks are capable to perform cognitive tasks such as pattern recognition and associative memory. Pattern recognition processes input data usually on the basis of *a priori* knowledge in form of a set of memorized patterns. An input pattern ξ^{inp} is then classified to whichever one of the stored p patterns $\{\xi^\mu\} = \{\xi^1, \dots, \xi^p\}$ it most closely resembles. Typical applications for pattern recognition include automatic recognition of objects and patterns in digital image analysis as well as voice and speech recognition. An associative memory is a system that completes *partially* known input pattern based on the stored content. Typical applications for associative memory include content-addressable memory as a special type of computer memory and database engines.

A classic theoretical model to perform the described tasks is a Hopfield network [2], a recurrent neural network with symmetric connections between individual neurons. Full connectivity is provided with every neuron i being able to interact with any other neuron $j \neq i$ by means of a response function $r_i(t) = \sum_{j \neq i} w_{ij} S_j(t)$ aggregated as a weighted sum over the current states of all other bipolar neurons $S_j(t) = \pm 1$ which correspond to biological states of not firing and firing electrical signals to its neighbour neurons. An activation function $f_i(x)$ of the neuron i then evaluates r_i in order to define if the neuron remains

in its current state or a state flip is applied, e.g. $S_i(t + \Delta t) = f_i(r_i)$ where $f_i(x) = \text{sgn}(x)$ is the sign function.

For a set of p patterns $\{\xi^\mu\}$ with $\mu = 1, \dots, p$ and bipolar $\xi_i^\mu = \pm 1$ different definitions for the synaptic connection strength w_{ij} between neurons i and j are possible, e.g. by (discrete) Hebbian matrix

$$w_{ij} = \frac{1}{N} \left[\sum_{\mu=1}^p \xi_i^\mu \xi_j^\mu - p \delta_{ij} \right] \quad (1)$$

which stores the memory information in a distributed manner with the maximum storage capacity of $p_{max} \cong 0.138N$ for N neurons. The input binary vector ξ^{inp} is imposed on the Hopfield network as its initial state. The dynamics of the system are designed in order to minimize a cost function

$$E(S, w, t) = -\frac{1}{2} \sum_{ij} w_{ij} S_i(t) S_j(t) \quad (2)$$

by converting the state of the network to a stable configuration which represents the recognized pattern. Thus, the physical background of the Hopfield model offers an approach for quantization of the neural network.

Quantum computers utilize special characteristics of quantum systems such as superposition and entanglement [3]. The corresponding algorithms provide computational effectiveness in comparison with classic routines for problems like search [4] and factorization [5]. Different hardware designs have been proposed for building a quantum computer, including liquid state NMR [6, 7, 8, 9] and ion traps [10]. The extensive technological development of NMR spectroscopy in the last five decades made it possible for NMR quantum computing to become a suitable test ground for novel quantum algorithms.

A formalization of computation using quantum adiabatic evolution leads to the concept of Quantum Adiabatic Computation (QAC) [11] that has been proven to

be equivalent to the standard network model of quantum computation [12]. Compared to the abstract computational language of the quantum networks model, QAC provides a more direct translation to experimental quantum computing.

The protocol for QAC is represented by a controlled Hamiltonian path $\mathcal{H}(s)$ with $s = \frac{t}{T} \in [0, 1]$ and running time T . The computational problem is encoded in the final Hamiltonian $\mathcal{H}(1) = \mathcal{H}_p$ and the solution of the computational problem corresponds to finding the ground state of \mathcal{H}_p . On the other side, the initial state of the quantum system $|\psi(0)\rangle$ is chosen to be an easily preparable ground state of $\mathcal{H}(0) = \mathcal{H}_i$. If the Hamiltonian is driven from \mathcal{H}_i to \mathcal{H}_p slowly enough, i.e. if the total calculation time T is chosen to be long enough, then in the adiabatic limit the final state of the quantum system comes arbitrarily close to the problem ground state. QAC can also be formulated in the framework of Quantum Annealing [13] utilizing a Hamiltonian trajectory

$$\mathcal{H}(s) = \Lambda(s)\mathcal{H}_i + \mathcal{H}_p \quad (3)$$

with $\Lambda(0)$ large enough to make \mathcal{H}_i the dominating term and $\Lambda(1) = 0$ which reduces the Hamiltonian to the constantly present contribution by \mathcal{H}_p . The transverse Hamiltonian \mathcal{H}_i represents the driver for the adiabatic evolution whereas the initial state $|\psi(0)\rangle$ of the annealing process is chosen so it corresponds approximately to an energy eigenstate of the initial Hamiltonian $\mathcal{H}(0) = \Lambda_{max}\mathcal{H}_i + \mathcal{H}_p$.

In classic terms, QAC represents minimization of an energy cost function. This offers a link from (usually irreversible) classic neural dynamics to quantum dynamics governed by unitary, reversible evolution.

In the following, we consider a quantum neural network with N neurons consisting of bipolar neural states -1 and $+1$ to be represented by a quantum system with N qubits in states $|0\rangle$ and $|1\rangle$. Whereas a classic artificial neuron can assume only a single 'fire'/'not fire' state at once, quantum neurons allow superpositions of these two states in the form of $\alpha|0\rangle + \beta|1\rangle$ with $|\alpha|^2 + |\beta|^2 = 1$.

We define the computational problem by means of a Hamiltonian

$$\mathcal{H}_p = \mathcal{H}_{mem} + \Gamma\mathcal{H}_{inp} \quad (4)$$

with \mathcal{H}_{mem} containing the knowledge about stored patterns, \mathcal{H}_{inp} representing the computational input and the type of the problem as well as an appropriate weight factor $\Gamma > 0$.

We consider the following options to represent the memory patterns. In analogy to the energy function (2), the memory Hamiltonian can be defined by the coupling strengths between the qubits

$$\mathcal{H}_{mem}^{coupl} = -\frac{1}{2} \sum_{i \neq j} w_{ij} \sigma_i^z \sigma_j^z \quad (5)$$

where σ_i^z is the Pauli z matrix on qubit i . This definition allows a more direct experimental implementation compared to alternative representations based on quantum search projection operators [14]

$$\mathcal{H}_{mem}^{proj1} = \mathbb{1} - \sum_{\mu} |\xi^{\mu}\rangle \langle \xi^{\mu}| \quad (6)$$

$$\mathcal{H}_{mem}^{proj2} = \mathbb{1} - |\xi^{mem}\rangle \langle \xi^{mem}| \quad (7)$$

with memory state

$$|\xi^{mem}\rangle = \frac{1}{\sqrt{p}} \sum_{\mu} |\xi^{\mu}\rangle \quad (8)$$

which extend the capacity of the network at the cost of requiring multilinear interactions between the neurons.

For the retrieval Hamiltonian \mathcal{H}_{inp} we consider a single input pattern ξ^{inp} of length N . For associative memory applications we can extend a noncomplete input vector $\hat{\xi}^{inp}$ of length $n < N$ by setting the values for $N - n$ unknown states to zero.

In contrast to the classic neural network, we impose the input pattern ξ^{inp} on the dynamics of the system by an additional Hamiltonian term \mathcal{H}_{inp} . This bias retrieval Hamiltonian for pattern recognition can be defined as

$$\mathcal{H}_{inp} = \sum_i \xi_i^{inp} \sigma_i^z. \quad (9)$$

The energy spectrum of \mathcal{H}_{inp} , i.e. the entries on the diagonal at the position corresponding to an arbitrary pattern ξ is given by $E^{inp}(\xi) = -n + 2\hat{h}$ and depends on the Hamming distance $\hat{h} = 0, \dots, n$ between $\hat{\xi}^{inp}$ and $\hat{\xi} = \{\xi_1, \dots, \xi_n\}$, i.e. the number of position for which the corresponding entries are different. Thus this external field creates a scalar metric which permits comparison of the similarity between input and memory by shifting the energy levels of the memory Hamiltonian \mathcal{H}_{mem} and removing the degeneracy of its ground state in favor of patterns whichever have the largest overlap with the input pattern. It can be furthermore shown that for the simple case of a single stored pattern ($p = 1$), the upper bound for the weight factor Γ in combination with the memory Hamiltonian $\mathcal{H}_{mem}^{coupl}$ (5) is given by $\Gamma < 1 - \frac{n}{2N}$. In combination with the projector memory Hamiltonian $\mathcal{H}_{mem}^{proj1}$ (6), the bound is $\Gamma < \frac{1}{2n}$ for an arbitrary value of p . The bounds have been checked empirically.

We can enable the measurement of similarity between stored patterns and the input patterns by combining (9) with the definition (7) for \mathcal{H}_{mem} . For this, we reinterpret probability measurement as a measurement of relevance. The bias retrieval Hamiltonian shifts equally distributed weights in the memory state (8) according to the corresponding Hamming distances. With $\hat{\xi}^i = \{\xi_1^i, \dots, \xi_n^i\}$, Hamming distance $\hat{h}_i = d_H(\xi^{inp}, \hat{\xi}^i)$ between $\hat{\xi}^i$ and the retrieval pattern, the final ground state is

$$|\psi_0^p\rangle \propto \sum_{\mu} \frac{1}{\sqrt{p}} \left[1 - 2\Gamma\delta\hat{h}_{\mu} \right] |\xi^{\mu}\rangle + O(\Gamma^2) \quad (10)$$

where $\delta\hat{h}_\mu = \hat{h}_\mu - \langle\hat{h}\rangle$ is the deviation of the Hamming distance from the average relative Hamming distance $\langle\hat{h}\rangle = \frac{1}{p} \sum_{\mu=1}^p \hat{h}_\mu$.

Finally, we define the initial conditions of the QAC protocol. We choose the initial state of the network to be

$$|\psi(0)\rangle \equiv |\psi_{un}\rangle = \frac{1}{2^{\frac{N}{2}}} \sum_{k=0}^{2^N-1} |k\rangle \quad (11)$$

representing a ‘blank memory’ with uniformly distributed probability for all possible state configurations. We can consider the structure of \mathcal{H}_{mem} in the choice of the initial Hamiltonian \mathcal{H}_i in Eq. (3). In the case of the coupling memory Hamiltonian (5), we choose $\mathcal{H}_i = \frac{1}{2} \sum_i (\mathbb{1} - \sigma_i^x)$ whereas in the case of the projector memory Hamiltonians \mathcal{H}_{mem}^{proj} it can be defined as a projector $\mathcal{H}_i = \mathbb{1}_N - |\psi_{un}\rangle\langle\psi_{un}|$.

In order to provide an experimental proof for the concept of quantum pattern recognition we use a two-qubits liquid state NMR quantum computer. In following, we employ the definitions provided by the coupling memory Hamiltonian (5) and bias retrieval Hamiltonian (9). We implement a flip-flop as the most simple Hopfield network with a single connection between two qubits, where $w = -1$ corresponds to patterns with different bit values and $w = +1$ to patterns with identical bit values. Following Eq. (4), the problem Hamiltonian is thus represented by

$$\mathcal{H}_p = -w\sigma_1^z\sigma_2^z + \Gamma \left(\xi_1^{inp}\sigma_1^z + \xi_2^{inp}\sigma_2^z \right). \quad (12)$$

The NMR free evolution Hamiltonian

$$\mathcal{H}'_p = 2\pi J\sigma_H^z\sigma_C^z + 2\pi\nu_H\sigma_H^z + 2\pi\nu_C\sigma_C^z \quad (13)$$

for the considered molecule shows a constant positive coupling. In order to implement variable memory weight w according to Eq. (12), we can map the problem by defining the offset frequencies $\nu_H = -w\Gamma J\xi_1^{inp}$ respectively $\nu_C = -w\Gamma J\xi_2^{inp}$ and redefining the (problem dependent) initial Hamiltonian $\mathcal{H}'_i = -w(\sigma_H^x + \sigma_C^x)$. The initial quantum state $|\psi_{un}\rangle$ approximately corresponds to the ground state of $\mathcal{H}(0)$ for $w = +1$ and to its highest excited energy eigenstate for $w = -1$. Our choice of ν_H and ν_C consequently encodes the desired $|\psi_{res}(w, \xi^{inp})\rangle$ as the ground state respectively the corresponding excited state of the Hamiltonian $\mathcal{H}(T)$. In classic terms, the first case represents minimization of a cost function whereas the second involves its maximization.

For the simulations and experiments, we considered a heteronuclear two spin system corresponding to the ^1H and ^{13}C nuclear spins $\frac{1}{2}$ of ^{13}C labelled sodium formate dissolved in D_2O . The experiments were performed at a temperature of 27°C using a Bruker AC 200 spectrometer operating at the Larmor frequency of 200 MHz for ^1H and 50 MHz for ^{13}C . The heteronuclear ^1H - ^{13}C coupling constant is $J = 195$ Hz and the relaxation times

are $T_1(^1\text{H}) = 1.6\text{s}$, $T_1(^{13}\text{C}) = 2.7\text{s}$, $T_2(^1\text{H}) = 130\text{ms}$, $T_2(^{13}\text{C}) = 60\text{ms}$.

Following Eq. (11), the desired initial state for the considered heteronuclear two spin system is $|\psi_{un}\rangle = \frac{1}{2}(|00\rangle + |01\rangle + |10\rangle + |11\rangle)$ corresponding to the density matrix $\rho_{un} = |\psi_{un}\rangle\langle\psi_{un}|$. Rewriting this density matrix in terms of spin operators, ignoring the identity term and proportional constants, the initial state can be represented by the simplified and traceless operator $\rho(0) = \sigma_H^x + \sigma_C^x + 2\sigma_H^x\sigma_C^x$. This state can be created starting from the thermal equilibrium using standard methods based on spatial averaging [15].

The transversal form of the initial Hamiltonian \mathcal{H}_i suggests that pulse sequences applied on the transverse direction x can be used not only to generate but also to effectively control the initial Hamiltonian. More specifically, \mathcal{H}_i is represented by a transverse radio frequency (rf) field in positive or negative (depending on w) x direction on both spins. The amplitude of rf field $\Lambda(t)$ is reduced linearly from $\Lambda(0) = A_{max}$ to $\Lambda(T) = 0$ during the fixed evolution time $T = 50\text{ms}$ which is shorter than relaxation times T_1 and T_2 . The offsets ν_H and ν_C in Eq. (13) were set to values $\pm 100\text{Hz}$ and 0Hz corresponding to values $\xi_i = \pm 1$ and $\xi_i = 0$, respectively.

In the simulations and experiments of quantum annealing, the time evolution of the system was discretized into L steps of length $\Delta t = T/L$ with constant Hamiltonian $\mathcal{H}(t)$ for the time interval $[t, t + \Delta t]$. The continuous evolution is approximated for $L \rightarrow \infty$ and $\Delta t \rightarrow 0$. Our empirical results suggest that $L = 100$ leads to sufficient accuracy. We chose $\Gamma = 0.5$ for the weight parameter of the retrieval Hamiltonian term. We set $A_{max} = 600\text{Hz}$, where we get a reasonable success probability of 98%.

The results of the quantum annealing is read out by applying $\frac{\pi}{2}$ pulses followed by detection of the ^1H or ^{13}C signals. The ^1H signal were acquired as single scan while ^{13}C signal were acquired using 16 scans. The spectra recorded after the read out are shown in Fig. 1. A reasonable match between the experimental results and simulations (data not shown) is found. The first and third columns represent ^1H spectra which encode the computational results as presented in Table I. The first four rows represent applications of associative pattern recognition with $n = 1$ and $N = 2$ where the algorithm evaluates the Hamming distance between the input and the partial memory patterns. A single peak at frequency $\nu_H \pm \frac{J}{2}$ corresponds to the unique recognized pattern. Its position and direction identify the pattern recognition results, e.g. left negative peak identifies the state $|-1, 1\rangle$ corresponding to the output pattern $[-1, 1]$. In case of the blank input pattern $\xi_1^{inp} = \xi_2^{inp} = 0$, the quantum neural network returns its memory content as consistent patterns $[-1, 1]$, $[1, -1]$ for $w = -1$ and $[-1, -1]$, $[1, 1]$ for $w = +1$. The resulting quantum state represents a superposition of pattern states identified by corresponding spectral peaks. For completeness, we show in the second

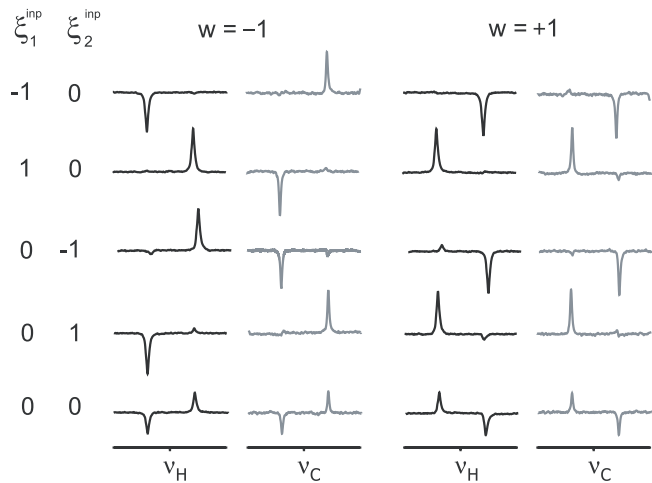


FIG. 1: Experimental ^1H and ^{13}C spectra for five combinations of ξ_1^{inp} and ξ_2^{inp} and two possible values of w , where $w = -1$ and $w = +1$ correspond to stored patterns with opposite and equal bit values, respectively. The spectral range in each spectrum is $\pm 240\text{Hertz}$.

ξ_1^{inp}	ξ_2^{inp}	$ \psi^{\text{out}}\rangle$ for $w = -1$	$ \psi^{\text{out}}\rangle$ for $w = +1$
-1	0	$ -1, 1\rangle$	$ -1, -1\rangle$
1	0	$ 1, -1\rangle$	$ 1, 1\rangle$
0	-1	$ 1, -1\rangle$	$ -1, -1\rangle$
0	1	$ -1, 1\rangle$	$ 1, 1\rangle$
0	0	$\frac{1}{\sqrt{2}}(-1, 1\rangle + 1, -1\rangle)$	$\frac{1}{\sqrt{2}}(-1, -1\rangle + 1, 1\rangle)$

TABLE I: The results of the pattern recognition represented by the corresponding pure quantum states.

and fourth column of Fig. 1 corresponding ^{13}C spectra. Peaks at $\nu_C \pm \frac{J}{2}$ provide redundant information to the identification of the patterns. In summary, we have developed a new theoretical approach for quantum pattern recognition and implemented it using liquid state NMR techniques.

In contrast to classic neural networks, a quantum neural register can represent a superposition of recognized patterns. Quantum superposition allows each of these patterns to be identified which is not the case for linearly combined mixture states in classic neural networks [1].

The projector memory Hamiltonian also allows a differentiation between stored patterns and their reversed patterns $-\xi^\mu$ in contrast to classic Hopfield network. The input pattern is imposed in form of an external physical field, which simplifies practical realization and offers prospects for nano-scale hardware implementation of a quantum neurocomputer. Since the problem is directly encoded into the final Hamiltonian \mathcal{H}_p , no ancilla qubits are required.

In the experiments, we realized the desired morph-

ing between the Hamiltonians using quantum annealing. This allowed us to exploit the experimentally available control terms and didn't require an iterative synthesis of the effective Hamiltonian trajectory [16]. Furthermore, we performed both ground and excited state QAC.

Several open questions remain and are subject of our current research, such as the maximum storage capacity. Future directions of research are the extensions to larger spin systems using liquid state NMR quantum computation and application of the developed techniques to alternative hardware designs, such as ion traps with magnetic field gradients [17] which have been already contextualized in the quantum neural research [18].

The authors thank Prof. Wilhelm Zwerger at TU München for his support. R.N. and R.S. acknowledge support by Thomas Runkler and in particular Prof. Bernd Schürmann who initiated the project at Siemens Corporate Technology. We thank Manoj Nimbalkar, Dr. Raimund Marx and Dr. Wolfgang Eisenreich for their help in NMR experimentation. S.J.G. acknowledges support by the EU project QAP as well as by the DFG through SFB 631. R.N. acknowledges financial support from Siemens AG.

-
- [1] S. Haykin, *Neural Networks: A Comprehensive Foundation* (Prentice Hall, 1998), 2nd ed.
 - [2] J. J. Hopfield, Proc. Nat. Acad. Sci. U.S.A. **79**, 2554 (1982).
 - [3] N. D. Mermin, *Quantum Computer Science: An Introduction* (Cambridge University Press, 2007).
 - [4] L. K. Grover, Phys. Rev. Lett. **79**, 325 (1997).
 - [5] P. W. Shor, SIAM J. Comput. **26**, 1484 (1997).
 - [6] D. G. Cory, A. F. Fahmy, and T. F. Havel, Proc. Natl. Acad. Sci. U.S.A. **94**, 1634 (1997).
 - [7] N. A. Gershenfeld and I. L. Chuang, Science **275**, 350 (1997).
 - [8] L. M. K. Vandersypen et.al., Nature **414**, 883887 (2001)
 - [9] R. Marx et.al, Phys. Rev. A **62**, 012310 (2000).
 - [10] J. I. Cirac and P. Zoller, Phys. Rev. Lett. **74**, 4091 (1995).
 - [11] E. Farhi et al., Science **292**, 472 (2001).
 - [12] D. Aharonov et.al., *Proceedings of the 45th Annual IEEE Symposium on Foundations of Computer Science*, 4251 (2004).
 - [13] G. E. Santoro and E. Tosatti, J. Phys. A: Math. Gen. **39** R393 (2006).
 - [14] J. Roland and N. J. Cerf, Phys. Rev. A **65**, 042308 (2002).
 - [15] E. Knill, I. Chuang, and R. Laflamme, Phys. Rev. A **57**, 3348 (1998).
 - [16] A. Mitra et.al., J. Magn. Reson. **177**, 285 (2005).
 - [17] F. Mintert and C. Wunderlich, Phys. Rev. Lett. **87**, 257904 (2001).
 - [18] M. Pons et.al., Phys. Rev. Lett. **98**, 023003 (2007).